Dissociation Dynamics of Energy-Selected $C_5H_{10}^+$ Ions

Willi A. Brand† and Tomas Baer*

Contribution from the Department of Chemistry, University of North Carolina, Chapel Hill, North Carolina 27514. *Received October 7, 1983*

Abstract: The fragmentation reactions of six $C_5H_{10}^+$ isomers loosing CH_3 and C_2H_4 have been investigated by using the photoelectron photoion coincidence (PEPICO) technique. Except for the 2-methyl-2-butene ion dissociation all precursors exhibit a two-component decay indicating that dissociation occurs from at least two distinct forms of molecular ions. The observation is rationalized in terms of competition between dissociation from the original ion structure and isomerization to a lower energy isomer subsequently decomposing at a slower rate. The latter isomer is identified as the 2-methyl-2-butene molecular ion. The comparison of the measured absolute rates with those predicted by the statistical theory (RRKM/QET) suggests that the transition-state switching model is necessary for a quantitative agreement.

It is well-known that the electron impact mass spectra of a number of isomeric C_5H_{10} molecules are very similar. Exceptions are cyclopentane (**1**) and 1-pentene (**2**), which both show an enhanced loss of C_2H_4,[1,2] while 2-pentene (**3**) and the branched species, 3-methyl-1-butene (**4**), 2-methyl-1-butene (**5**), and 2-methyl-2-butene (**6**), preferentially loose a methyl radical. Therefore, the aim of a number of mass spectrometric studies on C_5H_{10} isomers has been the development of methods to distinguish the different species. The $C_5H_{10}^+$ ions of low internal energy, such as the metastable ions which dissociate in the field-free regions of a double-focusing mass spectrometer, result in similar intensity ratios for the two dominant fragment ions $C_3H_6^+$ and $C_4H_7^+$.[3,4] On the other hand, ions of high internal energy, such as are produced in field ionization kinetics experiments,[5,6] dissociate rapidly and with distinguishable product ion branching ratios. These results indicate that isomerizations of the parent ions are in competition with direct dissociation.

A number of techniques are available for determining the structures of low-energy, and therefore nondissociating, ions. Levsen et al.[7] as well as McLafferty and co-workers[3] observed that the collisional activation spectra of the various pentenes are distinct enough to identify the isomers under investigation. Similarly Gross and co-workers[8] reported an ICR experiment where they identified the different neutral C_5H_{10} molecules on the basis of the corresponding ion's different reactivity with butadiene. More recently van der Hart et al.[9] published an ICR-photodissociation study of the $C_5H_{10}^+$ radical cations in which they were able to distinguish the linear, the cyclic, and the branched species. Interestingly they found two different kinds of molecular ions from each isomer with different reactivities toward the corresponding neutral precursor and different photodissociation cross sections, an observation for which they were not able to give a sound explanation.

In order to differentiate ionic isomers, it is often necessary to deposit a great deal of internal energy into the ion so that it will dissociate rapidly, and in a manner unique to its structure. One method of accomplishing this is by charge stripping. In this experiment, the parent ion is mass selected by the magnetic sector of the mass spectrometer. It is then collided at high translational energy (≈8 kV) with an inert gas such as He. The doubly charged fragment ions resulting from the collision are then analyzed with the electric sector. Because the doubly charged ion has typically 20 eV more internal energy than the singly charged ion, the technique is sensitive only to collision processes which deposit large amounts of energy. This is in contrast to the collision-induced dissociation (CID) or photodissociation experiments in which only 3–5 eV are typically transferred to internal energy. Miller and Gross[10] have investigated the charge-stripping spectra of ten $C_5H_{10}^+$ isomers and found that all could be distinguished. This implies that all ten isomers have sufficiently deep potential wells so that for each isomer a majority of the ions formed in the ion source maintain their structure.

Harrison et al.[11] performed an experiment in which the dissociation of pentene ions was studied in a range of energies, from threshold to several eV above the dissociation limit. They determined the breakdown graphs of the $C_5H_{10}^+$ molecular ions by measuring fragment ion ratios of energy-selected pentene ions using charge exchange mass spectrometry. The diagrams for the branched species were very similar and different from those for cyclopentane and 1-pentene, especially at high ion internal energies, thereby confirming the early EI results.

The conclusions from all these studies can be summarized as follows: the branched species 3-methyl-1-butene (**4**), 2-methyl-1-butene (**5**), and 2-methyl-2-butene (**6**), as well as 2-pentene (**3**), isomerize at low energies to a common structure prior to dissociation. Similarly, the molecular ions of cyclopentane (**1**) and 1-pentene (**2**) also isomerize in the metastable time region (microseconds), but they undergo specific reactions at shorter times. This is particularly evident in the charge-stripping spectra.[10] However, as we will show, the dissociation mechanism is considerably more complex. In our investigation of the C_5H_{10} isomers using energy selection of the molecular ions by photoelectron photoion coincidence (PEPICO[12]) spectroscopy, some interesting new aspects have emerged regarding the nature of the ions, as well as the applicability of RRKM/QET[13,14] to such a complex reaction system.

Experimental Procedure

The experimental setup was the same as the one described recently[15] and shall therefore be outlined here only briefly. Molecules are photoionized by monochromatic light, produced from a hydrogen discharge source and dispersed by a monochromator with a resolution of 2 Å. The ions are accelerated by a homogeneous electric field perpendicular to the photon beam, while the photoelectrons are accelerated in the opposite direction, energy selected by a threshold electron energy analyzer using

† Present address: Institut for Physikalische Chemie der Universitaet Bonn, 53 Bonn 1, F.R. Germany.

(1) Beynon, J. H.; Saunders, R. A.; Williams, A. E. "The Mass Spectra of Organic Molecules"; North-Holland Publishing Co.: Amsterdam 1968.
(2) Stenhagen, E.; Abrahamsson, S.; McLafferty, F. W. "Registry of Mass Spectral Data"; Wiley-Interscience: New York, 1974.
(3) Nishita, T.; McLafferty, F. W. *Org. Mass Spectrom.* **1977**, *12*, 75.
(4) Bowen, R. D.; Williams, D. H., *Org. Mass Spectrom.* **1977**, *12*, 453.
(5) Brand, W. A.; Stockloev, J.; Walther, H. J. *Int. J. Mass Spectrom. Ion Phys.*, submitted for publication.
(6) (a) Beckey, H. D. *Z. Naturforsch., A* **1961**, *16A*, 505. (b) Beckey, H. D.; Hey, H.; Levsen, K.; Tenschert, G. *Int. J. Mass Spectrom. Ion Phys.* **1969**, *2*, 101. (c) Levsen, K. "Fundamental Aspects of Organic Mass Spectrometry"; Verlag Chemie: Weinheim and New York, 1978.
(7) Levsen, K.; Heimbrecht, J. *Org. Mass Spectrom.* **1977**, *12*, 131.
(8) Gross, M. L.; Lin, P. H.; Franklin, S. J. *Anal. Chem.* **1972**, *44*, 974.
(9) Velzen, P. N. Th. v.; Hart, W. J. v. d., *Chem. Phys.* **1981**, *61*, 335.
(10) Miller, D. L.; Gross, M. L., *Org. Mass Spectrom.* **1983**, *18*, 239.
(11) Li, Y. H.; Herman, J. A.; Harrison, A. G. *Can. J. Chem.* **1981**, *59*, 1753.
(12) Baer, T. In "Gas Phase Ion Chemistry"; Bowers, M. T., Ed.; Academic Press: New York, 1979; Chapter 5.
(13) Marcus, R. A.; Rice, O. K. *J. Phys. Colloid. Chem.* **1951**, *55*, 894.
(14) Rosenstock, H. M.; Wallenstein, M. B.; Wahrhaftig, A. L., Eyring, H. *Proc. Natl. Acad. Sci. U.S.A.* **1952**, *38*, 667.
(15) Butler, J. J.; Baer, T. *J. Am. Chem. Soc.* **1980**, *102*, 6764.

0002-7863/84/1506-3154$01.50/0

Table I. C_5H_{10} Thermochemistry (kJ/mol) and Fragment Ion Appearance Energies (AE, eV)

isomer	$\Delta H_f°_{298}(C_5H_{10})^a$	E_{th},[b] eV	$\Delta H_f°_0(C_5H_{10})^c$	$C_4H_7^+$(PI)[d] AE_{298}	$C_4H_7^+$(EI)[e] AE_{298}	$C_3H_6^+$(PI)[d] AE_{298}	$C_4H_7^+$[f] E_0
1	−78.4 ± 0.8	0.075	−44.2 ± 0.8	11.15 ± 0.03	11.14	11.22 ± 0.04	10.76
2	−21.9 ± 1.2	0.120	+7.9 ± 1.2	10.63 ± 0.02	10.64	10.68 ± 0.02	10.83
3	−32.7 ± 0.9	0.120	−2.9 ± 0.9		10.68		10.77
4	−27.4 ± 0.6	0.113	+3.1 ± 0.6	10.75 ± 0.03	10.74	10.76 ± 0.05	10.87
5	−35.6 ± 0.7	0.113	−5.1 ± 0.7		10.85		10.91
6	−42.1 ± 0.6	0.113	−11.6 ± 0.6		10.84		10.86

[a] Data from ref 19. [b] Average C_5H_{10} thermal energy at 298 K. [c] Conversion to 0 K using standard procedures (see ref 20). [d] This study. [e] Data from ref 23. [f] Absolute 0 K energy = $AE_0 + \Delta H_f°_0(C_5H_{10})$.

the steradiancy principle,[16] and detected by a channeltron. The electrons serve as start pulses for the time-of-flight analysis of the coincident ions, accomplished by a time-to-pulse height converter and a multichannel analyzer. These data are transferred to, and analyzed by, a PDP-11/03 computer. Due to the coincident detection of the zero-energy electron with its corresponding ion, the internal energy, E, of the ion is completely determined by $E = h\nu$ - IP + E_{th}, where E_{th} is the average thermal energy of the C_5H_{10} molecule prior to photoionization. The distribution of this thermal energy causes some smearing of E as does the finite resolution of the steradiancy analyzer. Both effects can be corrected for in the data analysis.[17,18] The samples used in this study were the highest grade commercially available compounds, whose purity was checked by gas–liquid chromatography. No impurity exceeding 1% was detected.

Results and Data Analysis

A. Dissociation Limits and Breakdown Diagrams. The 298 K heats of formation of all six neutral C_5H_{10} isomers (Table I) are well-known.[19] In order to interpret the dissociation rates quantitatively, it is important to know the thermochemistry of all species at 0 K. These were determined from the 298 K values by the procedure previously outlined,[20] in which the average thermal energy is calculated from the C_5H_{10} vibrational frequencies. The latter were generated from those of 2-methylpropane.[21] The resulting 0 K values are listed in Table I and are used in constructing Figure 1.

The adiabatic ionization energies shown in Figure 1 were obtained from Rosenstock et al.[22] and verified in this study. The dissociation limits to $C_4H_7^+ + CH_3$ for all six isomers, measured by Lossing using monoenergetic electron ionization[23] (EI), are listed in Table I. We measured the onsets of photoionization (PI) for three of the isomers using either a quadrupole mass filter or ion time-of-flight analysis following pulsed electrostatic ejection of the ions from the ionization region. In general, the onsets were difficult to assign because they were not very sharp. But within the experimental uncertainty, the PI and EI onsets agree. By adding the average thermal energy for each isomer (Table I) we can determine a 0 K onset. If we now add to that the 0 K heats of formation of the neutral C_5H_{10}, we obtain the 0 K $C_4H_7^+$ onset on the absolute energy scale. These onsets are shown in the last column of Table I.

The sharpest $C_4H_7^+$ photoionization onset was found for the cyclopentane (**1**) ion. The value of 10.76 eV on the absolute 0 K scale was also the lowest onset observed for any of the pentene

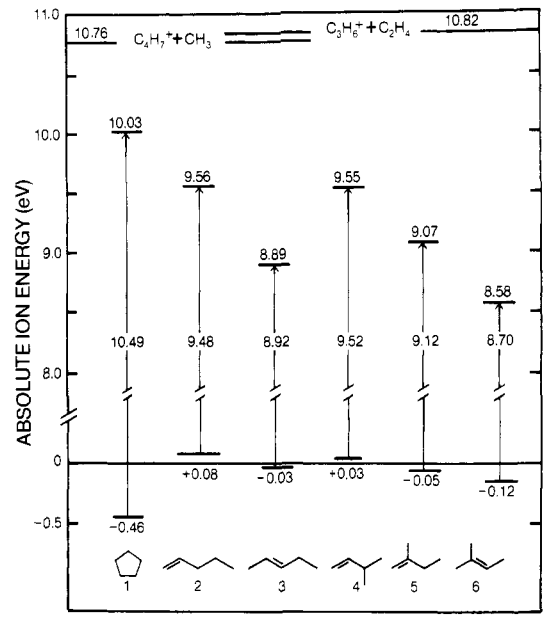

Figure 1. Energetics of the C_5H_{10} species on an absolute 0 K energy scale. For a discussion see Table I and text.

isomers (see last column of Table I). We accept this value as the correct dissociation limit for a number of reasons. First, **1** was found to dissociate rapidly at the dissociation limit so that it is not subject to a kinetic shift as is for instance 2-methyl-2-butene (**6**) which has a large activation energy. The kinetic shift is the shift in the observed dissociation onset as a result of the slow dissociation which prevents the detection of the fragment ion. Second, as will become evident, this set of isomers dissociates via a number of different routes, some of which involve rate-determining isomerizations. As a result, some of the reactions may proceed via reverse activation energies. Finally we note that the 0 K thermochemical dissociation limit for $C_3H_6^+ + C_2H_4$ is well established through the known 0 K heats of formation of these two products (983 and 60.7 kJ/mol, respectively). This calculated onset, on the absolute energy scale, is 10.82 eV. Now we note that the onsets for $C_3H_6^+$ and $C_4H_7^+$ from cyclopentane are shifted by 0.06 eV, so that we can determine a calculated dissociation onset for $C_4H_7^+$ of 10.76 eV, which agrees precisely with the measured onset from isomer **1**.

The 10.76-eV dissociation limit is equal to $\Delta H_f°_0(C_4H_7^+) + \Delta H_f°_0(CH_3)$. Using the tabulated CH_3 heat of formation of 145.6 kJ/mol we calculate $\Delta H_f°_0(C_4H_7^+)$ = 892 kJ/mol. Converting back to 298 K gives a value of 876 kJ/mol. This latter value is considerably higher than the 863 kJ/mol listed in Rosenstock's compilation[22] even though the experimental data providing the basis for these two values are essentially identical. The difference arises from the method of deriving heats of formation. The one outlined here, which takes into account the thermal energy, is now generally considered the correct approach. In addition, it is shown here that this approach is entirely consistent with the observed and calculated values for the dissocaiton onset of $C_3H_6^+ + C_2H_4$.

Since the internal energy of the ions is defined through the coincidence condition, the relative abundances of the parent and

(16) Baer, T.; Peatman, W. B.; Schlag, E. W. *Chem. Phys. Lett.* **1969**, *4*, 243.
(17) Brand, W. A.; Baer, T. *Int. J. Mass Spectrom. Ion Phys.* **1983**, *49*, 103.
(18) Werner, A. S.; Baer, T. *J. Chem. Phys.* **1975**, *62*, 2900.
(19) Sussex, N. P. L. "Computer Analysed Thermochemical Data"; Pedley, J. B., Rylance, J., Eds.; University of Sussex, 1977.
(20) (a) Fraser-Monteiro, M. L.; Fraser-Monteiro, L.; Butler, J. J.; Baer, T.; Hass, R. *J. Phys. Chem.* **1982**, *86*, 739. (b) Rosenstock, H. M. "Kinetics of Ion–Molecule Reactions"; Ausloos, P., Ed.; Plenum Press: New York, 1979; p 246. (c) Traeger, J. C.; McLaughlin, R. C. *J. Am. Chem. Soc.* **1981**, *103*, 3647.
(21) Shimanouchi, T. "Tables of Molecular Vibrational Frequencies, Consolidated"; Government Printing Office: Washington, 1972; NSRDS-NBS Vol. I.
(22) Rosenstock, H. M.; Draxl, K.; Steiner, B. W.; Herron, J. T. "Energetics of Gaseous Ions", American Chemical Society: Washington, 1977; J. Phys. Chem. Ref. Data, Vol. 6.
(23) Lossing, F. P. *Can. J. Chem.* **1972**, *50*, 3973.

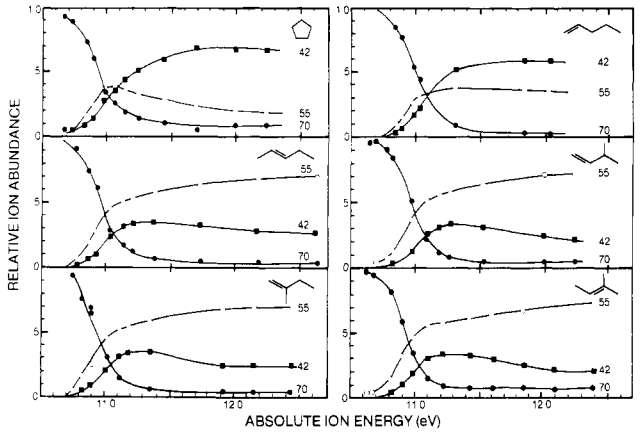

Figure 2. Breakdown graphs of $C_5H_{10}^+$ ions on an absolute 0 K energy scale measured with our PEPICO experiment for a maximum dissociation time of 5 μs. The diagrams are not corrected for thermal energy or hot electron contribution.

daughter TOF signals at different photon energies directly constitute a breakdown graph. Such breakdown graphs for $C_5H_{10}^+$ isomers, shown in Figure 2, confirm the charge exchange data of Harrison et al.[11] The choice of ion energy is not limited in PEPICO experiments as it is in charge-transfer preparation of ions so that our data points, particularly near the dissociation threshold, are more closely spaced. The diagrams for the branched species and 2-pentene are nearly identical with only small differences near the fragmentation threshold and in the ratio of mass 42 to mass 55 at high energies. These results indicate that at internal energies up to about 1.5 eV above the dissociation threshold, the branched species and 2-pentene isomerize nearly completely prior to dissociation. 1-Pentene and cyclpentane show the intensity ratios of the two major fragments reversed from what they were in the other isomers. However, there are some significant differences between the two breakdown graphs of **1** and **2**, indicating that isomerization prior to dissociation is not complete.

B. Dissociation Rates. In principle, the information about the rate constants could be drawn from the breakdown diagrams. However, the shape of the TOF distribution is more sensitive to the rate. The smearing out of the internal energy by the thermal internal energy and especially the steradiancy analyzer function affect the peak shapes less than the breakdown graph. Some of the coincidence time-of-flight distributions are shown in Figure 3. The asymmetry in the peaks arises from parent ions decomposing in the acceleration region. This is the basis for the extraction of the rate constant $k(E)$. Compared to "normal" fragment peak shapes in PEPICO spectroscopy (see for instance ref 24), which can be fit by using a single exponential decay function, the TOF distributions for $C_3H_6^+$ (m/z 42) and $C_4H_7^+$ (m/z 55) could be fit only by using at least two independent exponential rate functions with varying weight for each peak. The only exception was 2-methyl-2-butene (**6**) for which a single component fit was adequate. The solid lines in Figure 3 for isomers **1**, **3**, **4**, and **5** are therefore represented by two-component fits, while isomer **6** is fit with a one-component decay rate. Table II summarizes the experimental results for the different species.

The TOF distributions of the fragment ions from the six isomers are quite varied, some showing the two-component nature more obviously than others. If we regard the product TOF distributions of one parent ion, e.g., 1-pentene, at several internal energies (Figure 4) we see immediately that the reaction is very complicated. At 10.71 eV of absolute energy, 1-pentene evidently dissociates rapidly to $C_3H_6^+$, but only slowly to $C_4H_7^+$. This can only come about as a result of two different parent ions. The origin of these different parent ion structures will be discussed in the next section. It should be noted that Meisels et al.[25,26] recently

Table II. Dissociation Rates for $C_5H_{10}^+$ Ions in μs^{-1}

		m/z 55			m/z 42		
$h\nu$	E_{abs}	k_1	k_2	f_2	k_1	k_2	f_2
			Cyclopentane (**1**)				
11.06	10.68	3	0.1	0.1	3	0.1	0.03
11.12	10.74	5	0.2	0.12	5	0.2	0.03
11.24	10.86	10	0.2	0.25	10	0.2	0.03
11.29	10.91	10	0.2	0.25	10	0.2	0.03
11.39	11.01	10	0.45	0.45	10	0.45	0.06
11.44	11.06	10	0.6	0.6	10	0.6	0.06
11.52	11.12	10	1.0	1.0	10	1.0	0.06
			1-Pentene (**2**)				
10.63	10.83	10	0.2	0.3	10	0.2	0.01
10.68	10.88	10	0.2	0.4	10	0.2	0.04
10.69	10.89	10	0.25	0.5	10	0.25	0.05
10.78	10.98	10	0.4	0.25	10	0.4	0.04
10.83	11.03	10	0.5	0.6	10	0.5	0.06
			trans-Pentene (**3**)				
10.69	10.78	10	0.1	0.1		weak	
10.78	10.87	10	0.2	0.12	10	0.2	0.05
10.83	10.92	10	0.3	0.3	10	0.3	0.1
10.96	11.05	10	0.7	0.4	10	0.8	0.25
11.05	11.14	10	1.5	0.7	10	1.5	0.25
11.12	11.21	10	2.0	1.0	10	2.0	0.2
			3-Methyl-1-butene (**4**)				
10.55	10.69	1.6	0.1	0.03		weak	
10.64	10.78	1.8	0.1	0.15		weak	
10.68	10.82	3	0.2	0.35	3	0.2	0.3
10.83	10.97	5	0.4	1.0	5	0.4	0.5
10.95	11.09	10	1.0	0.4	10	1.0	0.4
11.04	11.18	10	1.0	0.2	10	1.5	0.2
11.12	11.26	10	2.0	0.6	10	2.0	0.3
			2-Methyl-1-butene (**5**)				
10.76	10.82	3	0.3	0.6	3	0.3	0.15
10.83	10.89	10	0.3	1.25	10	0.2	0.07
10.83	10.89	5	0.3	1.0	5	0.3	0.2
10.95	11.01	10	0.6	1.0	10	0.6	0.25
11.12	11.18	10	1.3	0.6	10	1.3	1.0
			2-Methyl-2-butene (**6**)				
10.69	10.68		~0.1			~0.1	
10.82	10.81		0.25			0.25	
10.92	10.91		0.5			0.5	
10.95	10.94		0.3			0.5	
11.00	10.99		0.35			0.6	
11.00	10.99		0.5			0.6	
11.12	11.11		1.1			1.3	
11.23	11.22		2.5			3.0	

noted a similar dual rate dissociation of CH_3ONO to NO^+ and CH_3O^+, which was attributed to non-interconverting electronic states.

Each TOF peak in Figures 3 and 4 can be fit with three parameters in eq 1 which are the two rates k_1 and k_2 and f, the fraction of dissociation events which decay via rate k_1. All three

$$\text{rate} = f\exp(-k_1t) + (1-f)\exp(-k_2t) \qquad \text{(I)}$$

parameters varied with photon energy. Such fits were performed for both mass peaks at all photon energies for the six isomers. It was possible to fit all the curves at a given absolute ion energy with a single pair of decay rates, k_1 and k_2. Of course the fraction, f, was not identical and in fact varied considerably from isomer to isomer (see Table II). The faster of the two rates was faster than we could measure (i.e., $k > 4 \times 10^6\ s^{-1}$) except perhaps near threshold. The lower of the two rates at each photon energy is plotted in Figure 5 as a function of the absolute energy. It is evident from Figure 5 that the slow rates are identical for all

(24) Baer, T.; Willet, G. D.; Smith, D.; Phillips, J. S. *J. Chem. Phys.* **1979**, *70*, 4046.

(25) Meisels, G. G.; Hsieh, T.; Gilman, J. P. *J. Chem. Phys.* **1980**, *73*, 4126.

(26) Gilman, J. P.; Hsieh, T.; Meisels, G. G. *J. Chem. Phys.* **1983**, *78*, 3767.

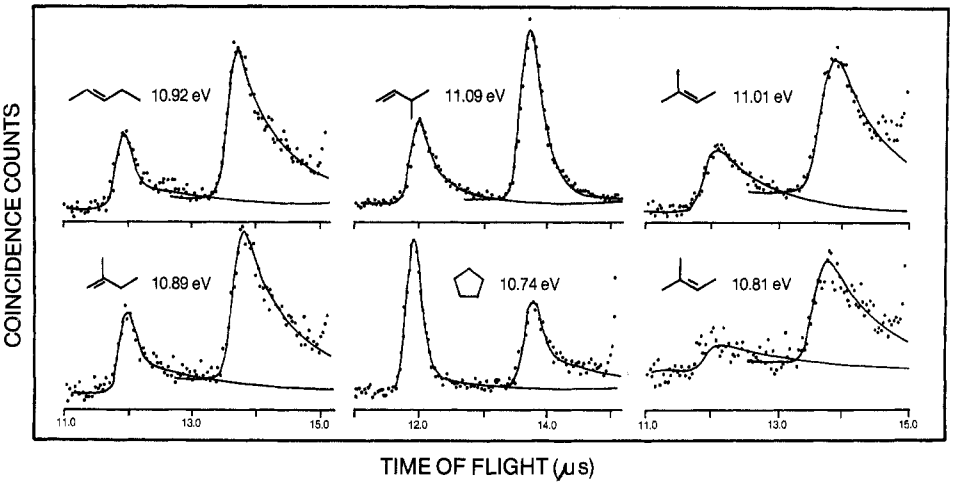

Figure 3. Some experimental time-of-flight distributions of the fragment ions $C_3H_6^+$ (12 μs) and $C_4H_7^+$ (13.8 μs). The parent ion (m/z 70) is not shown. The solid lines represent the double exponential fits (eq 1, in text) except for 2-methyl-2-butene where a single exponential was adequate. Energies are on an absolute scale.

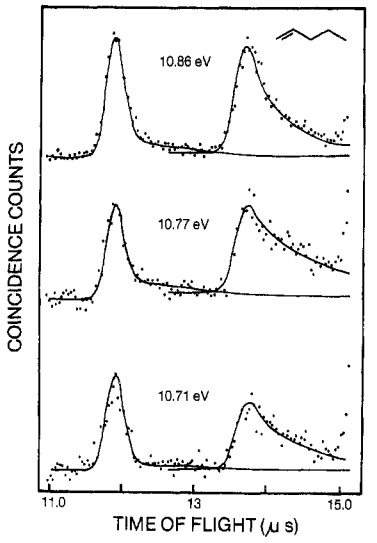

Figure 4. Time-of-flight distributions for 1-pentene at different internal energies. CH_3 is lost preferentially with a slow rate while C_2H_4 exceeds the time resolution of our experiment at the lowest energies measured.

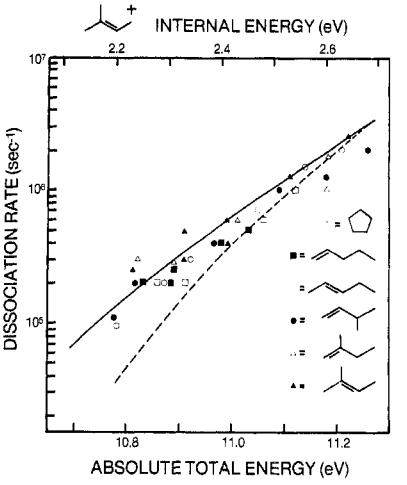

Figure 5. The slow experimental rates for all precursors, shown on a common energy scale. The two lines are RRKM/QET calculations. For the solid line, E_0 was 1.65 eV and the transition state was tight. For the dashed line, E_0 was 1.85 eV and the transition state was moderately loose.

isomers and that in addition the single exponential decay rates observed from 2-methyl-2-butene (**6**) match the observed points for the other isomers very well. The striking similarities and differences in the breakdown diagrams, the two-component rates, and the identical slow component dissociation rate all point to the conclusion that the C_5H_{10} isomeric ions have a strongly, but not completely, coupled dissociation mechanism.

Discussion

A. Origin of the Two-Component Decay. As demonstrated by the solid lines, the data of Figures 3 and 4 can be adequately fit by assuming a two-component decay. Of course, a three-component model with five adjustable parameters would fit the data better, and one could develope an appropriate mechanism for such a situation. However, two-component decays are rather rare, having been found so far only for $C_2H_5Cl^+$, $C_2H_4Cl_2^+$, $C_3H_3Cl^+$,[27,28] and possibly $C_4H_8^+$.[29] A three-component decay is very unlikely, and so we treat the present data in terms of the simplest model for a two-component decay.

There are several situations which give rise to two-component decay rates. All involve the existence of ultimately two distinct parent ions which decay via different rates. The various explanation differ in the assumed nature of these states and the mechanism for their production. One possibility is the direct formation of parent ions in two different, noninterconverting, electronic states which fragment at different rates. One of the dissociation rates may be slow because a formally forbidden curve crossing prevents the ion in one of the electronic states from directly fragmenting. Such a case has been suggested for the HCl loss from $C_2H_5Cl^+$[27] and CH_3 loss from CH_3ONO^+.[25,26] This situation is described by the two-component depletion rate for the molecular ion as given directly by eq I, in which f and $(1 - f)$ are the respective fractions of the two species formed in the initial ionization process and k_1 and k_2 are the rates at which the two states dissociate. The mechanism can be extended easily to more than one product ion. Another mechanism that results in fragment ions being produced from different electronic states is one in which an ion, formed initially in an excited electronic state, decays rapidly via two channels. These are (a) direct dissociation to products or (b) radiationless transitions or fluorescence to the ground electronic states. Clearly, the dissociation rate from the ground electronic state, even if the total energy is equal to that of the excited state, will be much slower. NO and NO_2 loss as well as NO^+ production from $C_6H_5NO_2^+$[30] appear to be examples of this mechanism in which part of the NO^+ and all of the NO_2 loss are

(27) Tsai, B. P.; Werner, A. S.; Baer, T. *J. Chem. Phys.* **1975**, *63*, 4348.
(28) Baer, T.; Werner, A. S.; Tsai, B. P. *J. Chem. Phys.* **1975**, *62*, 2497.
(29) Baer, T.; Smith, D.; Tsai, B. P.; Werner, A. S. In "Advances in Mass Spectrometry"; Daly, N. R., Ed.; London, 1977; 7A, p 56.
(30) Panczel, M.; Baer, T. *Int. J. Mass Spectrom. Ion Phys.*, in press.

Tabler III. $C_5H_{10}^+$ Molecular Ion[a] Frequencies (cm^{-1}) Used in the RRKM/QET Calculation

3000	2950	2900	1660	1470	1420	1365	1065	800	385
2970	1460	1075	980	193	3090	2980	2890	1460	1380
1280	1045	975	430	2950	1440	1080	890	430	196
3000	3000	1350	1350	1350	1350	1300[b]	300	200	

[a] The same frequencies were assumed for the tight transition state. Two 1350-cm^{-1} frequencies were reduced to 300 cm^{-1} for moderately loose transition state. [b] Assumed reaction coordinate.

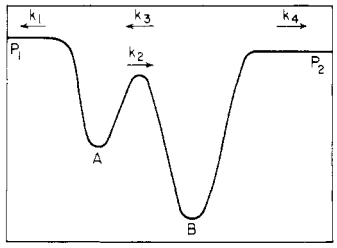

Figure 6. Model potential for a competitive dissociation/isomerization reaction.

formed by direct dissociation, while vibrationally excited ground electronic state ions, formed by radiationless transitions, dissociate slowly to produce part of the NO^+ and all of the NO loss products.

The observation of dissociation from excited electronic states (isolated states) has been limited to the above-mentioned examples as well as some small halogen-substituted alkanes such as $C_2F_6^+$,[31,32] $C_2H_4F_2^+$,[33] CF_3Cl^+,[34] and some of the monohalomethane ions.[35] For $C_5H_{10}^+$, an ion that is known to isomerize, the occurrence of isolated states seems rather unlikely. In fact there is not a single hydrocarbon ion in which isolated states have been detected so far. The reason for the rare occurrence of isolated states in ions is that the radiationless transition rates are generally faster than the direct dissociation rate. This also accounts for the small number of ion types which are known to fluoresce.[36] Nevertheless, competition between direct dissociation from an excited state and a radiationless transition to the ground state cannot be ruled out in most of the pentenes because the photoelectron spectra of, for instance, 1-pentene[11,37] and some of the other isomers[38] show that we initially form the ion in an excited electronic state. However, in the case of cyclopentane, the ionic dissociation limit lies in the first PES band[39,40] so that dissociation must be occurring exclusively from the ground electronic state. Therefore, we cannot invoke an isolated state in this ion. Yet, the rates are two component.

An alternative explanation, and one that appears most likely for the case of the C_5H_{10} isomers, is that a series of isomerization steps are in competition with dissociation. The expected overall rates for complicated dissociation mechanisms have been derived in a previous publication,[41] and therefore we quote here only the final expressions for the two-component decay.

Consider the model potential shown in Figure 6. The ion A formed upon ionization can decompose directly to the products P_1 at a rate k_1. However, in competition with this direct dissociation, A can isomerize to the more stable ion B with a rate k_2. This ion can now either dissociate to give the products P_2 with the rate k_4 or convert back to isomer A with a rate k_3 and decay to the products P_1. The fragments P_1 and P_2 need not be different; they could be the same products. Obviously, the observable rates depend on the relative magnitudes of the various rates, k_i. According to ref 41, three cases can be distinguished.

Case A: Isomerization Is Faster Than Dissociation ($k_2 \gg k_3 \gg k_1 \approx k_4$). This leads to a single exponential decay rate which is simply $k_1 + k_4$ because the whole system is at equilibrium and dissociates with one rate. This is the situation that is most frequently encountered in isomeric systems that isomerize.

Case B: Dissociation and Isomerization Are in Competition ($k_1 \approx k_2 \gg k_3 \approx k_4$). Under these circumstances the rates of formation for the two products P_1 and P_2 are given by:

$$\frac{d(P_1)}{dt} = k_1(A) = k_1\left[\frac{k_3}{k_1 + k_2}e^{-\lambda_- t} + \frac{k_1 + k_2}{k_2}e^{-\lambda_+ t}\right]$$

$$\frac{d(P_2)}{dt} = k_4(B) = k_4[e^{-\lambda_- t} - e^{-\lambda_+ t}]$$

where

$$\lambda_+ = k_1 + k_2 + \frac{k_2 k_3}{k_1 + k_2} \approx 2k_1 \qquad \text{(fast)}$$

$$\lambda_- = k_3\,\frac{2k_1 + k_2}{k_1 + k_2} \approx \tfrac{2}{3}k_3 \qquad \text{(slow)}$$

If we make the further simplification that $k_1 = k_2$, we get

$$\frac{d(P_1)}{dt} = \frac{k_3}{2}e^{-(2/3)k_3 t} + 2k_1 e^{-2k_1 t}$$

$$\frac{d(P_2)}{dt} = k_4[e^{-(2/3)k_3 t} - e^{-2k_1 t}] \approx k_4 e^{-(2/3)k_3 t} \qquad \text{for } t > 0$$

As is evident, products P_1 are formed with two-component rates, and the terms in the equation are easily related to the phenomenological eq I. On the other hand, the products P_2 will be formed at the single slow rate, $^2/_3k_3$, at times other than t near zero, because the second exponential term will rapidly vanish.

Case C: Initial Formation of the Lowest Energy Isomer ($k_1 \approx k_2 \gg K_3 \approx k_4$). The rates, $\lambda_\pm$, are identical with those in case B, but now (A)($t = 0$) = 0 so that P_2 now is formed at the same slow rate as is P_1. The most stable isomer therefore should always decompose with a single rate constant representing the overall depletion rate of the precursor.

The composite peak shapes we observe in the $C_5H_{10}^+$ decomposition find their explanation in case B dissociation except for 2-methyl-2-butene (**6**), the most stable isomer which shows single exponential decay, as predicted by the rates for case C. In both cases the slow component is identical with the depletion of ion B and therefore is evidence for the full isomerization of all precursors to a common structure at long times (Figure 5).

B. Two-Component Dissociation Rates and RRKM/QET Calculations. The striking feature of the TOF data of Figures 3 and 4, and the extracted decay rates shown in Figure 5, is that all ions fragment with the same slow rate. Of the six isomers investigated, the lowest energy structure is that of 2-methyl-2-butene (**6**) with an absolute energy of 8.58 eV. It would therefore be expected that all other isomers convert to this ion and that the slow rate is the rate of dissociation from this structure. This expectation is confirmed by the observation that all isomers except **6** show a two-component decay rate. Isomer **6**, being the lowest energy one, should not have a fast component, and in fact it does not. These differences are seen in the TOF data of Figure 3.

(31) Simm, I. G.; Danby, C. J.; Eland, J. H. D. *Int. J. Mass Spectrom. Ion Phys.* **1974**, *14*, 285.
(32) Inghram, M. G.; Hanson, G. R.; Stockbauer, R. *Int. J. Mass Spectrom. Ion Phys.* **1980**, *33*, 253.
(33) Stadelmann, J. P.; Vogt, J. *Int. J. Mass Spectrom. Ion Phys.* **1980**, *35*, 83.
(34) Powis, I. *Mol. Phys.* **1980**, *39*, 311.
(35) Eland, J. H. P.; Frey, R.; Kuestler, A.; Schulte, H.; Brehm, B. *Int. J. Mass Spectrom. Ion Phys.* **1976**, *22*, 155.
(36) Maier, J. P. *Angew. Chem., Int. Ed. Engl.* **1981**, *20*, 638.
(37) Hoshino, H.; Tajima, S.; Isogai, F.; Tsuchiya, T. *Bull. Chem. Soc. Jpn.* **1977**, *50*, 3103.
(38) Masclet, P.; Grosjean, D.; Mouvier, G.; Dubois, J. *J. Electron Spectrosc. Rel. Phenom.* **1973**, *2*, 225.
(39) Bieri, G.; Burger, F.; Heilbronner, E.; Maier, J. P. *Helv. Chim. Acta* **1977**, *60*, 2213.
(40) Potts, A. W.; Streets, D. G. *J. Chem. Soc., Faraday Trans. 2* **1974**, *70*, 875.
(41) Baer, T.; Brand, W. A.; Bunn, T. L.; Butler, J. J., *Faraday Discuss.* **1983**, *75*.

In attempting to calculate the statistical theory dissociation rate of **6** with the RRKM/QET program,[42] it became evident that the dissociation of 2-methyl-2-butene is not a simple one. If the energy difference between $C_4H_7^+ + CH_3$ (10.76 eV) and structure **6** (8.58 eV) is used as an activation energy (E_0 = 2.18 eV), the predicted rates at 11.0 eV are 3 orders of magnitude lower than the ones experimentally observed. No adjusting of frequencies (Table III) within reasonable bounds could bring both the slope and the magnitude of the calculated rates in accord with those in Figure 5. However, by lowering the activation energy from 2.2 to 1.65 eV and by employing a tight transition state it was possible to get excellent agreement with the experimental results (solid line in Figure 5). By assuming an E_0 or 1.85 eV and reducing two of the 1350-cm^{-1} frequencies to 300 cm^{-1}, it was possible to obtain a somewhat worse, but still satisfactory, agreement (dashed line). The disagreement at low energies is thought not to be too important because the thermal energy spread of our ions causes our experimental rates to be too high near the dissociation onset at 10.78 eV.

It is always possible to explain a rate faster than predicted by the statistical theory, by assuming that the ion is dissociating from an excited electronic state or that not all the vibrational frequencies are taking part in the energy randomization. However, given that we have a system of isomers that appear to interconvert rather freely, it seems most unlikely that either of these explanations are reasonable. On the other hand, a possible explanation for the fact that the RRKM/QET value for E_0 is lower than the thermochemical dissociation energy is that structure **6**, on its path toward dissociation, rearranges to a predissociating structure from which the dissociation is rapid. We can make use of the potential energy diagram of Figure 6. Suppose that ion **6** is structure B, and that the rate k_4 =0, so that all the dissociation must proceed via structure A. If the two transition states are such that $k_1 \gg k_2$, the rate of product formation will be given by

$$\frac{d(B)}{dt} = \left[k_3 - \frac{k_2 k_3}{k_1 + k_2} \right](B) \approx k_3(B)$$

This means that the isomerization is the rate-determining step and that the activation energy of 1.65 eV refers to this isomerization. The obvious structure for isomer A would be 2-methyl-1-butene (**5**) which can loose a CH_3 directly to form the most stable $C_4H_7^+$ product ion. However, this does not appear to be the case because ion **5** directly prepared by photoionization has a significant slow component (see Table II), that is, it rapidly reacts to form the lower energy structure, **6**. This is contrary to the assumption of a fast dissociation from isomer A. In addition, the activation energy for the direct dissociation of **5** is 1.71 eV, which is far too large to allow for a fast reaction. Rather, structure A would have to be some other intermediate with an energy near 9.5 eV. Yet, given that the $C_4H_7^+$ structure is that of the 2-methylallyl ion, there is no obvious precursor isomer other than **5**. It is interesting that a similar explanation has been proposed and similar problems in finding the intermediate structure were encountered for the dissociation of the butadiene ion.[43] We attempted to calculate the energy of structure A by varying it while searching for the condition that $k_1 > k_2$. The energies of the products, the isomer B, and the barrier between A and B were fixed, while the frequencies of the two transition states were varied. However, even when extreme parameters for the transition states were used, the isomerization of structure A over the barrier at 10.25 eV was always faster than its direct dissociation over the 10.76-eV margin. This means that the proposed isomerization prior to the dissociation mechanism for the 2-methyl-2-butene fragmentation is not very likely. The basic problem is that the energy gap between the isomerization barrier and the dissociation limit is too great to be compensated for by the usual loose complex.

(42) The Hase–Bunker program was used with the semiclassical Whitten–Rabinovitch state counting option. This program is available as No. 234 through the Quantum Chemistry Program Exchange, Indiana University.

(43) Jarrold, M. F.; Bass, L. M.; Kemper, P. R.; van Koppen, P. A. M.; Bowers, M. T. *J. Chem. Phys.* **1983**, *78*, 3756.

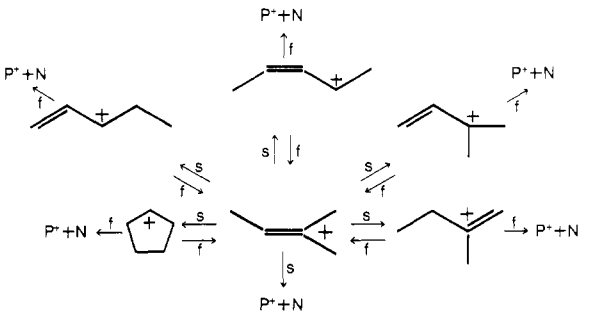

Figure 7. Schematic reaction scheme for the $C_5H_{10}^+$ dissociation (f = fast, s = slow).

In addition, we cannot propose an obvious structure for isomer A.

Chesnavitch et al.[44] recently proposed a transition-state switching model in which it was pointed out that different transition states, or phase space bottlenecks, are applicable depending on the energy of the ion. This treatment of the statistical theory has the effect of giving lower slopes in the $k(E)$ vs. E curve and provides a justification for using activation energies smaller than the E_0 expected on the basis of the thermochemistry. The transition-state switching model predicts that at high $C_5H_{10}^+$ internal energy, the bottleneck in the phase space corresponds to an energy well below the dissociation limit, so that above about 11 eV absolute energy, the lower E_0 along with a tight transition state is appropriate. This would correspond to the solid line in Figure 5. However, close to threshold, the bottleneck in the phase space is an orbiting one and the appropriate E_0 is the dissociation limit of 2.18 eV. However, this orbiting transition state is characterized by a number of free internal rotors, so that the rate of dissociation is orders of magnitude higher than it would be for a tight transition state. We have not actually carried out the calculations for the transition-state switching model because that would be beyond the scope of this work.

C. Mechanism for Coupled Isomerization Dissociation. The model potential of Figure 6 is a gross simplification of the actual potential energy surface of the $C_5H_{10}^+$ system. It neglects all details of the actual reaction pathways. It simply contains the feature that the isomerization barriers are lower than the first dissociation limit in accord with the finding that the metastable ion spectra of all precursors are identical. A somewhat more complete picture is provided in Figure 7 in which each of the outer isomers corresponds to an ion A in Figure 6 while the central 2-methyl-2-butene ion represents ion B for all cases. Although more complete than the curve of Figure 6, Figure 7 also neglects any details of the isomerization or dissociation pathways.

From one point of view, the pentenes divide into two groups: one of them containing cyclopentane and the linear species while the second group includes the branched species. Within each group, isomerization can take place via H shifts alone. The breakdown diagrams are in accord with this division except for 2-pentene which appears to have more in common with the branched isomers than with cyclopentane (**1**) and 1-pentene (**2**).

It is, however, very difficult to construct a complete diagram for all isomerization and dissociation reactions active in the unimolecular $C_5H_{10}^+$ chemistry. There are only a few reactions that we can assign with some confidence. Reactions 1 and 2 are

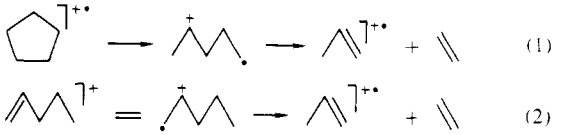

(1)

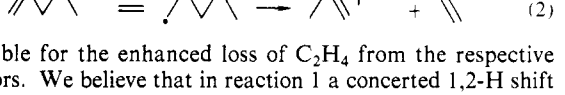

(2)

responsible for the enhanced loss of C_2H_4 from the respective precursors. We believe that in reaction 1 a concerted 1,2-H shift occurs, because otherwise, a primary cation would be involved

(44) Chesnavitch, W.; Bass, L.; Sue, T.; Bowers, M. T. *J. Chem. Phys.* **1981**, *74*, 2228.

imposing too large a barrier. The second reaction is a McLafferty rearrangement which is known to be a fast and facile process. The common feature in these two reactions is the radical site at one terminal end of the ion. It is, in fact, not possible to construct a simple bond cleavage from any $C_5H_{10}^+$ structure to give $C_3H_6^+$ and C_2H_4 without having the radical site on the terminal end of the precursor. This may be the reason why 1-pentene and 2-pentene behave so differently. 2-Pentene easily looses CH_3 via reaction 3. From the thermal isomerization chemistry of radicals

(3)

it is known that hydrogen rearrangements take place via 5- or 6-membered rings.[45,46] For the isomerization of the 1-hexyl to the 2-hexyl radical, a threshold energy of 12.6 kcal/mol was obtained from an RRKM fit to the rate data.[47] The same researchers found an activation energy of 19 kcal/mol for a 1,4-H shift in pentyl radicals. 1,5- and 1,3-H shifts have not been observed in these radicals indicating that the activation barrier was at least larger than 34 kacl/mol. Therefore, 2-pentene, in competition with reaction 3, is believed to undergo a 1,4-H shift leaving the radical site at the terminal end from which it can easily loose C_2H_4.

In the branched species, the reactions are the ones that account

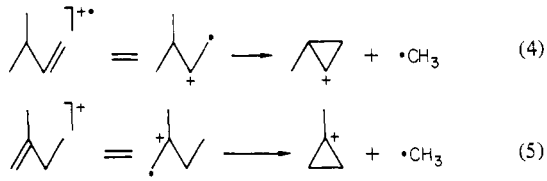

(4)

(5)

for the preferential loss of CH_3 over C_2H_4. At low energies, the latter may be lost after an isomerization to 2-pentene, a rearrangement involving CH_3 migration.

This discussion concerning the overall mechanism only deals with some fragmentary aspects of an overall complex reaction scheme. A more complete analysis is beyond the scope of this work. It will probably require more information, some of which may come from isotopic labeling studies. In addition, future investigations in our own laboratory, using cold molecules formed in a supersonic expansion, may provide more precise dissociation rate data from which additional mechanistic details can be derived.

Conclusion

In this analysis of the time of flight distribution of energy-selected C_5H_{10} ions, we have shown that the dissociation of these ions is characterized by two-component decay rates which is a result of a complex isomerization scheme. The enhanced loss of C_2H_4 from 1-pentene and cyclopentane ions, a process evident in the mass spectra of these molecules, is a result of a more or less direct dissociation which dominates at high ion internal energy. At energies near the dissociation threshold, a fraction of these ions isomerize to the most stable isomer, 2-methyl-2-butene. Dissociation from this stable isomer is slow because of the large activation energy. The identical slow dissociation rate component of all the isomers indicates that all parent ions partially isomerize to the 2-methyl-2-butene ion.

A comparison of the calculated statistical theory rate with the experimental dissociation rate of 2-methyl-2-butene indicates that the effective activation energy, E_0, is 0.4 ± 0.1 eV less than the thermochemical dissociation energy of 2.18 eV. This is another example of a reaction that requires the transition-state switching model. It is significant that the three systems in which the lowering of the nominal activation energy is apparent are all unsaturated hydrocarbon ions in which the rates have been measured near the dissociation energy.

Acknowledgment. We are grateful to Richard Kamens and Barbara Brand of the Department of Environment Sciences and Engineering for carrying out the GLC analysis. In addition we are indebted to Steen Hammerum, Karsten Levsen, and Lewis Bass for helpful discussions. Finally, W.A.B. thanks the Deutsche Forschungsgemeinschaft for a post-doctoral fellowship. This work was supported by a grant from the National Science Foundation.

Registry No. 1, 287-92-3; **2**, 109-67-1; **3**, 109-68-2; **4**, 563-45-1; **5**, 563-46-2; **6**, 513-35-9.

(45) Hardwidge, E. A.; Larson, C. W.; Rabinovitch, B. S. *J. Am. Chem. Soc.* **1970**, *92*, 3278.
(46) Larson, C. W.; Chua, P. T.; Rabinovitch, B. S. *J. Phys. Chem.* **1972**, *76*, 2507.
(47) Watkins, K. W. *J. Phys. Chem.* **1973**, *77*, 2938.
(48) Watkins, K. W.; Larsen, D. R. *J. Phys. Chem.* **1975**, *75*, 1632.